Nucleation Behavior of *n*-Alkane Microdroplets in an Electrodynamic Balance†

I. Weidinger, J. Klein, P. Stöckel, and H. Baumgärtel*

Institut für Physikalische und Theoretische Chemie, Freie Universität Berlin, Takustrasse 3, 14195 Berlin, Germany

T. Leisner

Institut für Physik, TU Ilmenau, Postfach 100565, 98684 Ilmenau, Germany

Received: February 26, 2002; In Final Form: December 30, 2002

The nucleation behavior of *n*-alkane droplets with carbon numbers ranging from 14 to 17 was observed in an electrodynamic balance. Changes in the elastic light-scattering pattern of the single levitated microdroplets indicate the phase transition from liquid to solid. Cooling/heating experiments showed larger supercooling temperatures than expected for alkane droplets with an alkane/air interface. Measurements of the nucleation rates of $C_{15}H_{32}$ and $C_{17}H_{36}$ gave additional information about the dynamics of the nucleation process and allowed us to distinguish homogeneous from heterogeneous nucleation.

1. Introduction

The effect of supercooling is a well-known phenomenon for almost all liquids. In contrast to melting, which usually occurs close to the thermodynamic phase-transition temperature T_m, most liquids freeze at a much lower temperature T_k if cooled for a finite rate. The maximum supercooling temperature $\Delta T = T_m - T_k$ is not a constant but depends on the cooling rate and the sample volume. It is therefore more precise to refer to the nucleation rate $J(T)$, which is the rate of formation of solid-phase nuclei per unit time and volume. $J(T)$ is substance-specific and usually a very steep function of temperature. Supercooling occurs because the creation of a solid nucleus involves the formation of a new interface between the solid and liquid phases. The free energy of a spherical nucleus of radius r is therefore given by

$$\Delta F(r) = 4\pi r^2\sigma - \frac{4}{3}\pi r^3 \Delta S\, \Delta T \qquad (1)$$

Here, σ represents the interface energy, ΔT is the supercooling below the equilibrium melting temperature, and ΔS is the entropy of melting per unit volume. $\Delta F(r)$ has a negative contribution from the bulk free-energy difference between the liquid and solid phases and a positive contribution from the interface energy. The stability of the nucleus depends on the change in free energy upon the addition of another monomer. A nucleus for which $\delta F_r/\delta r = 0$ is called a critical nucleus or germ, and its free energy ΔF_g is the nucleation barrier. Smaller nuclei tend to dissolve whereas larger nuclei grow and lead to the freezing of the whole sample. In the simplest form of classical nucleation theory,[1] the nucleation rate J is is related to ΔF_g by

$$J = \frac{N_e kT}{h} \exp\left(-\frac{\Delta F_g + \Delta F_{act}}{kT}\right) \qquad (2)$$

Here, ΔF_{act} is the activation energy for adding a single molecule to the nucleus. N_e stands for the number of molecules per unit volume, and h stands for the Planck constant. This equation allows us to determine ΔF_g from measured nucleation rates if ΔF_{act} is derived from viscosity data.

The thermodynamics of the *n*-alkanes C_nH_{2n+2} has been of major interest in the literature since they are some of the simplest nonpolar organic molecules and are often used as models for chainlike molecular systems. Their freezing behavior, however, is remarkably complex.[2−11] Although bulk samples with $n > 13$ can hardly be supercooled at all,[7,9] emulsified samples exhibit a significant supercooling temperature ΔT that depends strongly on chain length.[2,3,9] For the short alkanes, ΔT decreases with increasing carbon number, undergoes a minimum around $n = 17$, and then increases again. This behavior was explained by the results of surface tension[4] and X-ray scattering investigations[5] of the liquid alkanes. They reveal the formation of a solid monolayer at the alkane/air interface a few degrees above its melting temperature for carbon numbers $14 < n < 50$. This monolayer was assumed to serve as an ideal nucleus for heterogeneous crystallization. At the alkane/water interface in emulsions, this monolayer is not necessarily formed, and homogeneous nucleation is invoked.

In this paper, we introduce a third kind of measurement: the observation of mean supercooling temperatures and the evaluation of nucleation rates of *n*-alkane droplets trapped in an electrodynamic balance. These droplets exhibit an alkane/air interface but do not have any wall contact that could serve as a freezing nucleus. We present results for alkanes with carbon numbers from 14 to 17.

Alkanes in this size range with odd numbers of carbons nucleate into a so-called rotator phase. This high-temperature solid phase exhibits long-range order in the molecular axis orientation but lacks long-range order in the rotational degree of freedom of the molecules about their long axis.[12,13] They pass through a second solid−solid phase transition a few kelvins below where an orthorhombic crystal is formed.[14,15] The alkanes with even numbers of carbons, however, crystallize into a

† Originally submitted to the "R. Stephen Berry Festschrift", published as the November 4, 2002, issue of *J. Phys. Chem. A* (Vol. 106, No. 45).

* Corresponding author. E-mail: baum@chemie.fu-berlin.de.

10.1021/jp0205362 CCC: $25.00
Published on Web 03/26/2003

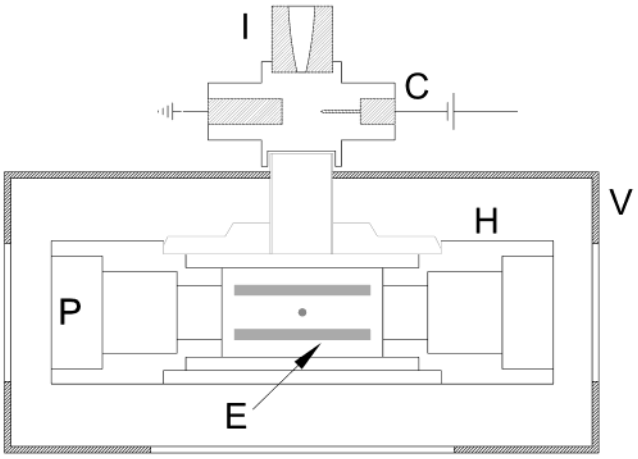

Figure 1. Experimental setup. I: injector, C: corona charging, P: ports, E: ring electrodes, H: copper housing, V: vacuum chamber.

triclinic phase.[16] For $C_{16}H_{34}$, nucleation into the triclinic phase via a transient rotator phase was observed.[8]

For alkanes, the expression for ΔF_g (eq 1) has to be modified because the assumption of a spherical nucleus is not valid for chainlike molecules. The simplest possibility is to assume a cylindrical nucleus with different surface energies at the side (σ_s) and the end (σ_e) of the molecule. The free energy ΔF can then be formulated as

$$\Delta F(r, l) = 2\pi r^2\sigma_e + 2\pi rl\sigma_s - \pi r^2 l\Delta S\,\Delta T \qquad (3)$$

Here, r and l stand for the radius and length of the germ, respectively. At a fixed size, the nucleus will minimize its free energy under the constraint that l is not smaller than the length of one molecule l_0. For alkanes, $l = l_0$ has been found to yield the minimum energy.[2,9] Under these conditions, ΔF_g is given by the following equation:

$$\Delta F_g = \frac{\pi l_0^2\,\sigma_s^2}{\Delta S\,\Delta T l_0 - 2\sigma_e} \qquad (4)$$

Only one layer of molecules stacked side by side forms the critical nucleus.

2. Experimental Section

2.1. Apparatus. The alkanes were purchased commercially from Sigma-Aldrich. The purity is better than 99%.

Levitated single droplets of average radius $r = 30\ \mu$m have been trapped in an electrodynamic balance.[17,18] Detailed information on this apparatus was published earlier.[19,20] The balance consists mainly of two ring electrodes with a high AC voltage applied. In addition, a DC voltage is superposed to compensate for the gravitational force on the droplet. From this voltage, the charge-to-mass ratio of the droplet can be obtained. The electrodes are surrounded by an octagonal copper chamber with eight ports for optical and electrical access to the trap. (See Figure 1.) To adjust and control the temperature, two flat copper disks cover the top and the bottom of the copper chamber. They can be cooled by liquid nitrogen and heated resistively. An outer vacuum chamber ($p = 10^{-4}$ to 10^{-5} mbar) surrounds the whole setup for thermal insulation. The temperature in the inner chamber is measured via two Pt 100 resistance thermometers, one being in contact with the copper housing and the other one being immersed in the gas phase near the ring electrodes. Differences of less than 0.04 °C between these two thermometers were observed at typical cooling rates below 1 °C/min. Copper housing and the gas phase are therefore always in thermodynamic equilibrium, and temperature gradients, which will cause gas convection, are negligible. A systematic temperature error of $\Delta T = 0.25$ °C was estimated from uncertainties in the calibration procedure. Temperature differences can be resolved better than $\Delta T = 0.02$ °C.

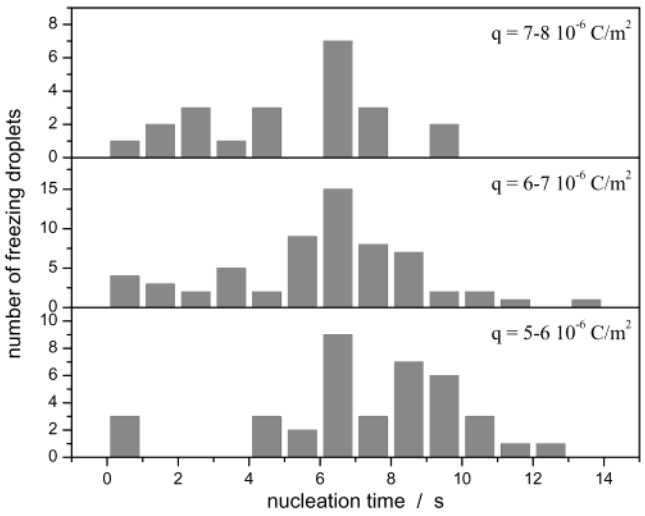

Figure 2. Distribution of the freezing times for several surface charge densities.

Single droplets were produced at room temperature by a homebuilt piezoelectric injector that is mounted on the top of the trap chamber as shown in Figure 1. They are injected vertically into the trap chamber that is kept at the temperature of interest. The time of thermalization has been calculated according to the following equation:[21]

$$(T(t) - T_\infty) = (T_0 - T_\infty)\exp\left(-\frac{4\pi r_0\lambda_u}{c_p M_{dr}}t\right) \qquad (5)$$

T_0 is the temperature at the start, and T_∞ is the temperature at the end of the thermalization. r_0 denotes the droplet radius, and M_{dr}, its mass. λ_u stands for the thermal conductivity of the surrounding medium (i.e., air) and c_p for the heat capacity of the droplet. The so-derived thermalization of the droplet from room temperature to 0 °C is fast and 99.9% complete after 0.08 s.

In our previous experiments[19,20,22,23] on aqueous solutions, the droplets have been charged by induction. However, nonpolar liquids such as alkanes have to be charged externally.[24,25] This can be done with the help of a corona discharge[26] between the injector nozzle and the trap. A sharp needle mounted opposite to a grounded plate is kept on a high negative potential ($U = -3$ kV). Under these conditions, a discharge current of a few microamperes of negative-charge carriers is observed.[27] Right after its ejection, the droplet passes this ionic current and acquires a surface charge density of about -7×10^{-6} C/m^2. It is not a priori clear if this surface charge has an influence on the droplet nucleation. We therefore studied the influence of the surface charge on the distribution of nucleation times (Figure 2). In the range of -5×10^{-6} to -8×10^{-6} C/m^2, this distribution remains unchanged. We therefore conclude that the small surface charge (1 e$^-$ in 10^5 surface molecules) has no influence on the nucleation. In addition, we performed freezing experiments with charged and uncharged bulk samples of

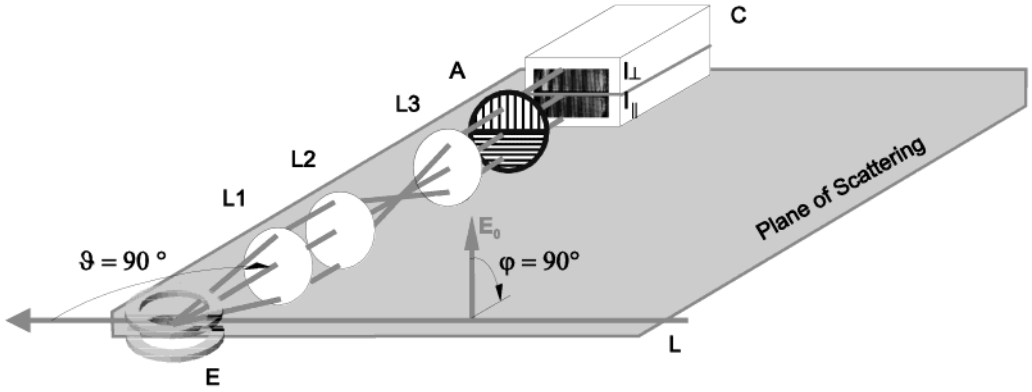

Figure 3. Optical setup. L: He−Ne laser beam, E: ring electrodes, L1−L3: lenses, A: analyzer, C: CCD camera.

alkanes on an insulating glass substrate. The probes have been prepared by collecting several thousand charged and uncharged droplets from the droplet generator. With the resulting flat hemispheres ($d \approx 5$ mm), neither for charged nor uncharged probes has supercooling within an error of ±0.5 °C been observed. Freezing occurred at the melting point of the bulk probe.

Inside the trap, the droplet is illuminated by a He−Ne laser ($\lambda = 632$ nm), which is polarized perpendicular to the plane of scattering. We observe the angular distribution of the scattered light in the range between 80 and 100° with a CCD camera. A schematic overview of the optical setup is given in Figure 3. The scattered light passes through a polarization separator (A) that maps the light parallel to the scattering plane in the upper half of the camera and perpendicular to the plane in the lower half of the camera (C). Figure 4a and b shows the angular resolved scattering pattern of a liquid and a solid droplet, respectively. The liquid droplet shows characteristic, almost equidistant stripes in the polarization channel of the incident laser beam. This interference pattern can be analyzed by using Mie theory, which describes the scattering of light by an ideal sphere.[28−31] The mean angular distance of two intensity maxima at a given index of refraction is approximately a linear function of the diameter d of the sphere. Therefore, if the index of refraction is known, then a linear calibration function can be calculated, and the diameter of the droplets can be determined online. Deviations from the linear dependence and uncertainties in the determination of the stripe distance lead to a systematic error of about 8% in the determination of d. The temperature-dependent indices of refraction for alkanes $C_{14}H_{30}$ to $C_{17}H_{36}$ were taken from the literature[32] for the H_α line (656.3 nm) and were extrapolated to lower temperatures.

If the incident laser beam is either completely parallel or perpendicular to the plane of scattering, then no depolarization will occur for an ideal sphere. This is clearly the case for the liquid droplet in Figure 4a. If nucleation occurs, then the droplet will lose its spherical symmetry. As one can see in Figure 4b, the characteristic stripes disappear, and the intensity in the depolarized channel increases strongly. This change is used to determine the moment of freezing.

2.2. Experimental Procedure. Two types of measurements were performed on the single levitated droplets. In the first type, a droplet was injected into the trap a few degrees above its melting temperature. The temperature was then decreased until the phase transitions occurred. Subsequently, the temperature was increased again until the particle melted. The intensity in the depolarized channel was used to detect the phase transitions (Figure 5).

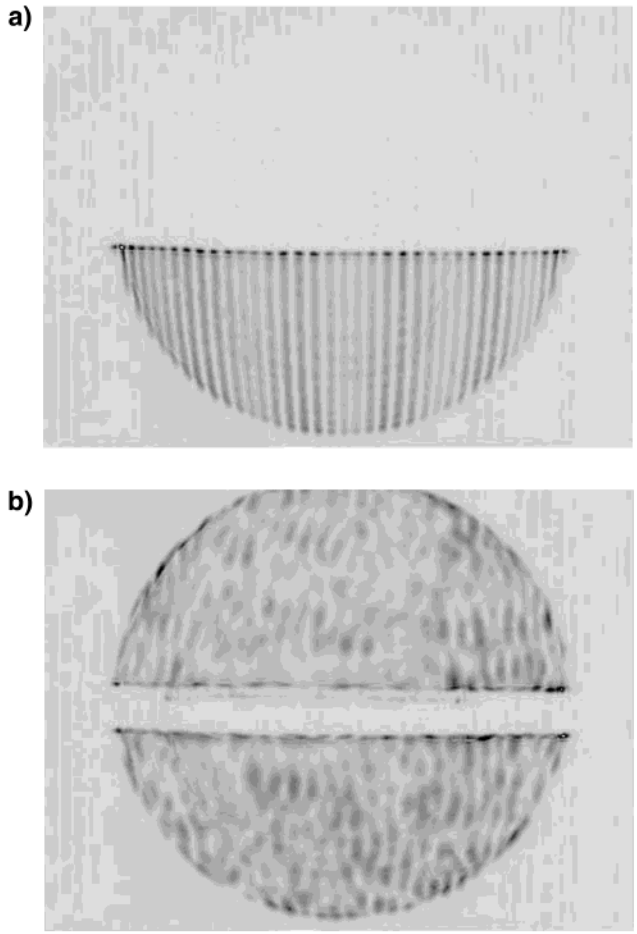

Figure 4. Scattering pattern for a (a) liquid and a (b) solid $C_{15}H_{32}$ droplet. The intensities are inverted for clarity.

To determine the nucleation rates, a second type of measurement was performed. The temperature was held at a constant value in the supercooled region where nucleation occurs on a reasonable time scale. Several hundred droplets were injected successively, and for each of them, the time until freezing was measured. Part of a typical series containing several hundred droplets is given in Figure 6. The intensity of the parallel and perpendicular channels is displayed as a function of time. The increase in the channel of the incident laser beam denotes the existence of a new droplet in the trap, and the increase in the second depolarized channel indicates the nucleation event. In the following, the time between these two events is called the nucleation time t_n. The homogeneous nucleation rate of the

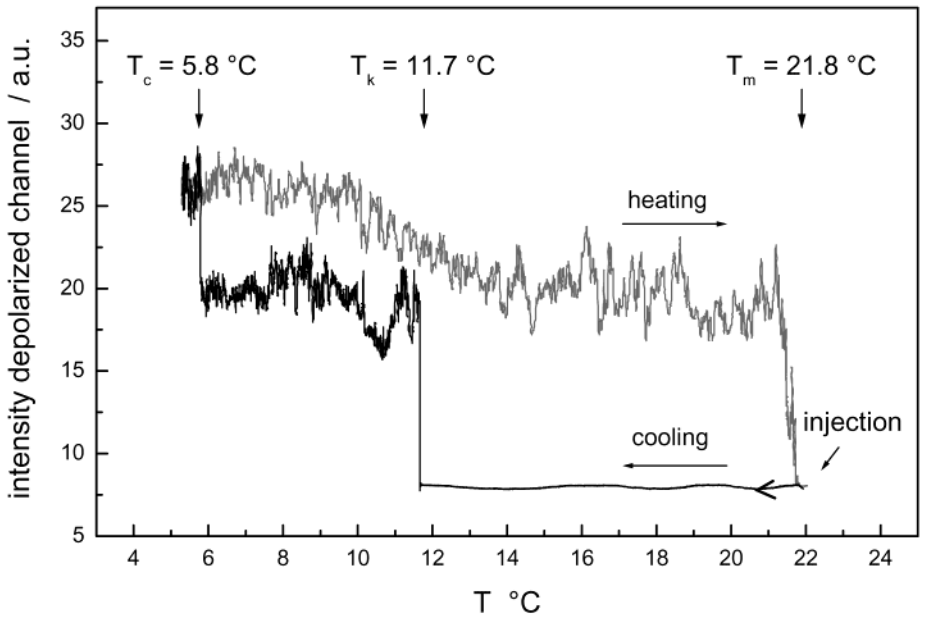

Figure 5. Intensity of the scattered light polarized perpendicular to the incident laser beam during a cooling/heating cycle of a $C_{17}H_{36}$ droplet.

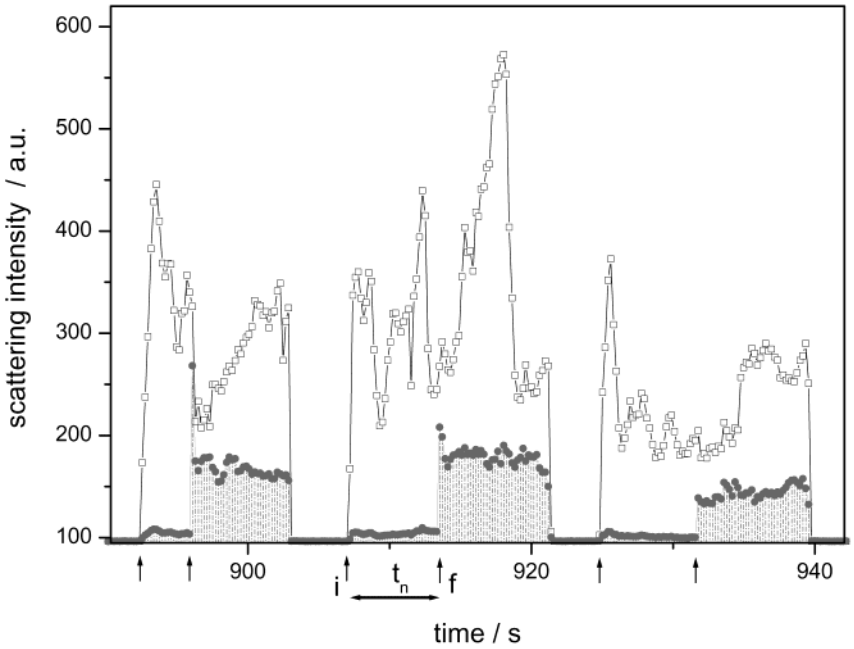

Figure 6. Typical measurement of nucleation times for $C_{15}H_{32}$. A sequence of three injection events out of several hundred is shown. Intensity polarized parallel (□) and perpendicular (●) to the incident laser beam: i, injection point; f, freezing point; t_n, nucleation time.

whole droplet ensemble is generally derived by the following equation:[33,34]

$$\ln\left(\frac{N_u}{N_0}\right) = -J(T)\, V t_n \tag{6}$$

N_u is the number of droplets that are still liquid after a certain time t, and N_0 is the total number of droplets observed. The natural logarithm of the ratio of these two values is proportional to the nucleation rate J times the product of the droplet volume V and its nucleation time t_n. A plot of the left-hand side of eq 6 versus Vt_n should produce a straight line. A typical example is given in Figure 7 for $C_{17}H_{36}$ at $\Delta T = 9$ °C. The experimental data fit on a straight line, indicating statistical nucleation according to eq 6. The slope of the line indicates the nucleation rate J. Measurements at various temperatures yield the temperature dependence of $J(T)$. This kind of analysis was done successfully in former trap experiments with droplets of water and sulfuric acid.[19,20,23]

However, some readers may get the impression that the data in Figure 7 could be better fit by two linear sections with a sharp crossover at $Vt_n = 1 \times 10^{-4}$ cm^3 s. It should therefore be mentioned that eq 6 represents the special case of homogeneous nucleation with a time-independent volume. A more general equation given in its differential form is

$$\frac{dN_u}{dt} = -\sum J_i(T)\, V(t)\, N_u \tag{7}$$

which takes into account that i different nucleation mechanisms with different nucleation rates J_i and time-dependent volumes V_i exist. Different slopes may result in systems where at least

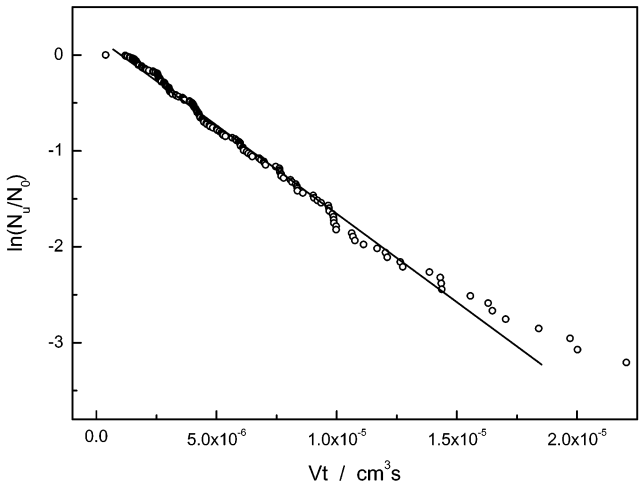

Figure 7. Nucleation plot for $C_{17}H_{36}$ at $\Delta T = 9$ °C.

TABLE 1: Phase-Transition Temperatures (°C) of Alkanes Analyzed in This Work[a]

n	T_m	T_{or}	T_l	T_k	T_c	ΔT_{dr}	ΔT_b	ΔT_{ems}
14	5.3			−5.4		10.7	2.94[b]	17.0[e]
15	10.1	−5	11.2	0.9	−8.0	9.2	0.31[b]/0.05[c]	13.5[d]
16	17.9		19.9	9.2		8.7	2.20[b]/1.85[c]	15.2[d]/14.6[e]
17	21.8	10	23.8	13.9	6.1	7.9	0.13[b]/0.03[c]	13.4[c]/13.6[e]

[a] T_m is the melting temperature and T_{or} is the temperature of the rotator/orthorhombic phase transition.[14] T_l is the temperature at which a solid surface layer is formed.[6] T_k and T_c are the temperatures at which the liquid/rotator and rotator/orthorhombic phase transitions, respectively, were observed in this work. $^{\Delta}T_{dr}$, $^{\Delta}T_b$, and $^{\Delta}T_{ems}$ are the supercoolings reached in this work, in bulk samples, and in emulsion samples, respectively. [b] Reference 7. [c] Reference 9. [d] Reference 2. [e] Reference 3.

two nucleation mechanisms with different time behavior of the corresponding volume occur. This volume is then not necessarily the total volume of the droplet but the volume containing the molecules that participate in the formation of the critical germ. If different nucleation mechanisms have to be considered, then different volumes have to be assigned to each mechanism. An example of this behavior is given below.

3. Results and Discussion

3.1. Supercooling Temperatures. We measured mean supercooling temperatures for alkanes with carbon numbers from 14 to 17 (Table 1). A typical example is given for a cooling/heating cycle of $C_{17}H_{36}$ in Figure 5. The cooling rate in this case was 0.46 °C/min. The liquid-to-solid phase transition occurs at 11.7 °C, which is 10.1 °C below its thermodynamic melting point.[38] On further cooling, the solid−solid phase transition from the rotator to the orthorhombic phase can be seen by a further increase in the intensity of the depolarized light. This second transition is also supercooled. In this case, it occurred at 5.8 °C, 4.2 °C below its equilibrium transition temperature. Heating of the droplet shows a smooth decrease in intensity starting at 10 °C and reaching a plateau at 14 °C. The intensity above 14 °C is identical to that observed for the rotator phase during the cooling cycle. Because the equilibrium temperature for the orthorhombic/rotator phase transition is exactly 10 °C, the decline between 10 and 14 °C can be related to a back transformation into the rotator phase. The heating rate in this case was 1.01 °C/min and was then reduced to 0.2 °C for $T >$ 21.5 °C. At 21.8 °C, melting of the solid droplet was observed. From this kind of measurement, supercooling temperatures of

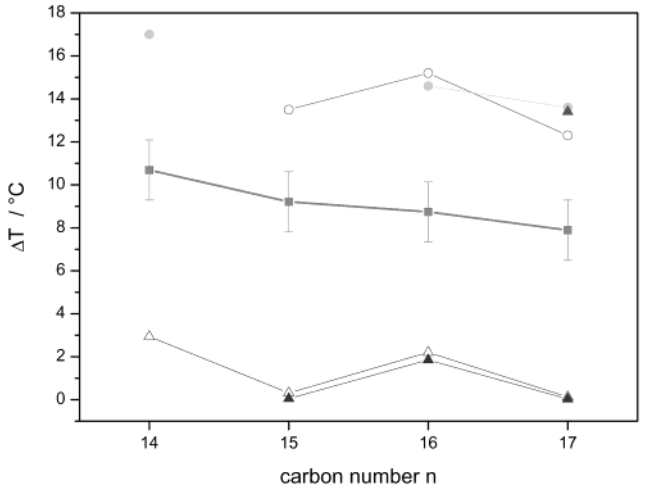

Figure 8. Supercooling temperatures reached in emulsions (▲: ref 9, ○: ref 2, ●: ref 3), single droplets (■: this work), and bulk solutions (▲: ref 9, △: ref 7).

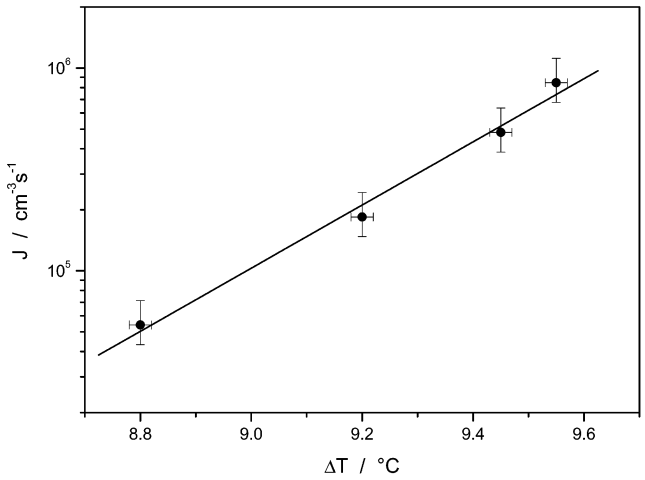

Figure 9. Temperature dependence of the nucleation rate of $C_{17}H_{36}$.

the liquid/solid and solid/solid phase transitions can be derived. In Figure 8 , ΔT is plotted as a function of *n* and compared with literature data of bulk solutions and emulsions. The error bars in this plot are not experimental uncertainties but are due to the statistical behavior of the freezing process, different droplet diameters (43.4−90.3 μm), and different cooling rates (0.20−1.07 °C/min). In contrast to the results of the bulk experiments, levitated alkane droplets with a liquid/air interface can be supercooled substantially. However, they could not be supercooled as low as emulsion samples. This is not surprising since the droplets in the emulsion samples were much smaller ($d_{mean} \approx 4$ μm) than the levitated droplets ($d_{mean} \approx 60$ μm). Therefore, a simple comparison of supercooling temperatures is not adequate.

For samples with different volumes V_1 and V_2, homogeneous nucleation is observed on a similar time scale (cf. eq 6) if

$$J(\Delta T_1)V_1 = J(\Delta T_2)V_2 \tag{8}$$

To compare the observed supercooling temperatures, one needs the temperature dependence of the nucleation rate. Assuming homogeneous nucleation, this dependence was measured exemplarily for $C_{17}H_{36}$ using the second kind of experiment. The nucleation rates of different temperatures are shown in Figure 9. The temperature dependence is described by $\mathrm{d} \ln J/\mathrm{d}T = 3.6 \pm 0.27$ °C^{-1}. Compared to water, where

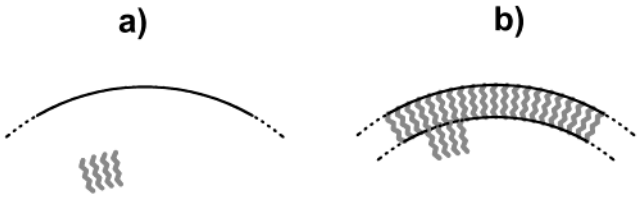

Figure 10. Nucleation mechanisms for a) homogeneous and b) heterogeneous nucleation.

d ln J/dT = 4.6 °C^{-1} was found,[19] this is a less-steep temperature dependence. From this result and eq 8, supercooling temperatures for emulsion samples and droplets are expected to differ by 2.3 ± 0.2 °C. The mean supercooling temperature for levitated droplets of $C_{17}H_{36}$ was ΔT = 7.9 ± 1.4 °C. Kraack et al.[9] stated a value of ΔT = 13.4 ± 0.5 °C for emulsions. Hence, the observed temperature difference is about 5.5 ± 1.9 °C. The larger supercooling values obtained in emulsion experiments can therefore be explained not only as an effect of smaller droplet volumes. It is very surprising, however, that we find better agreement between the droplets and the emulsions than with the bulk samples. The different nucleation behavior of emulsified and bulk samples was previously attributed to the existence of a solid monolayer at the liquid/air interface of the latter.[4,6] The formation of this solid monolayer decreases the surface tension. Levitated droplets also have an alkane/air interface Will this monolayer also be formed in these droplets since the charge and the curvature of the surface affect the surface tension? The increase in vapor pressure that results from increasing curvature is known as the Kelvin effect. It becomes important for droplets with radius r < 1 μm. Curvature-dependent surface tension is expected for even smaller droplets. This effect can therefore be neglected. The decrease in surface tension due to the excess charge is calculated to be $\Delta\gamma$ = 0.09 mN/m, which is also negligibly small. Therefore, we conclude that there is no reason that the formation of this monolayer should be suppressed. Then we have to assume that alkane droplets can be supercooled even in the presence of a solid surface monolayer. This is supported by Riegler et al.,[35] who observed supercooled liquid droplets of $C_{30}H_{62}$ in contact with their solid monolayer phase without immediate nucleation.

3.2. Surface Crystallization. If a stable surface layer is formed, then the germ can be generated heterogeneously at the interface between the liquid and the surface layer (cf. Figure 10b). The change in free energy ΔF in the case of heterogeneous nucleation is given as

$$\Delta F = \sigma_{s,l} A_{s,l} + (\sigma_{N,s} - \sigma_{N,l}) A_{N,s} + V \Delta S\, \Delta T \qquad (9)$$

with $\sigma_{s,l}$ as the interface energy between liquid and solid, $\sigma_{N,s}$ as the interface energy between substrate and solid, and $\sigma_{N,l}$ as the interface energy between substrate and liquid. $A_{s,l}$ and $A_{N,s}$ are the areas between liquid and solid and substrate and solid, respectively. In the case of an alkane droplet with a solid shell, we have $\sigma_{N,l} = \sigma_e$ and $\sigma_{N,s} = 0$. No end surface energy σ_e is required anymore. Therefore, eq 4 reduces to

$$\Delta F_g^{het} = \frac{\pi l_0 \sigma_s^2}{\Delta S\, \Delta T} \qquad (10)$$

In contrast to homogeneous nucleation (Figure 10a), where all molecules inside the droplet can participate in the formation of a critical nucleus, in heterogeneous nucleation only the molecules at the interface form the critical nucleus. The volume in eq 6 reduces to the droplet surface times the length of one molecule. Higher nucleation rates are therefore needed to arrive at our experimentally determined freezing probabilities. From these, one can directly calculate the free energy of germ formation from eq 2 and, subsequently, the surface energy σ_s using eqs 4 and 10, respectively. ΔF_{act} = 16.9 kJ/mol was estimated from the approximation given by Pruppacher et al.[1] $\Delta F_{act} = k(\partial(\ln(\eta/T))/\partial(1/T))$. The temperature dependence of the viscosity is given by Reid et al.[36] ΔS = 0.505 J/K cm^3 and σ_e = 1.09 mN/m for $C_{17}H_{36}$ were taken from Kraack et al.[10] For l_0, the usual approximation l_0 = 1.27 Å × n was made.

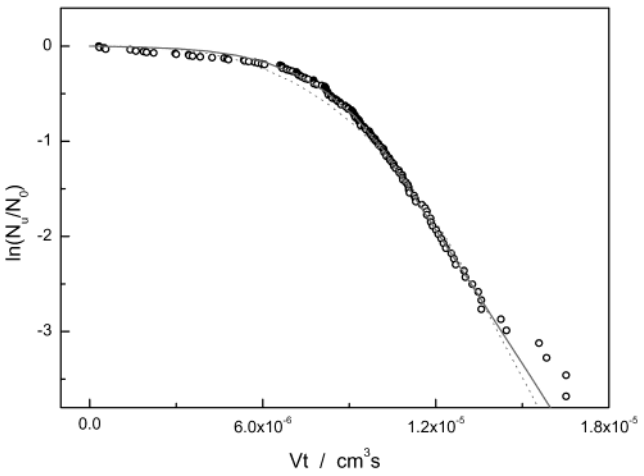

Figure 11. Nucleation plot for $C_{15}H_{32}$ at ΔT = 9.1 °C. The fits are according to eq 12 with n = 2 (···) and n = 3 (—).

TABLE 2: Nucleation Rates, ΔF_g, and σ_s of $C_{17}H_{36}$ Assuming Homogeneous and Heterogeneous Nucleation

		homogeneous			heterogeneous		
T_k °C	ΔT °C	J 10^5 cm^{-3} s^{-1}	ΔF_g kJ/mol	σ_s mN/m	J 10^{10} cm^{-3} s^{-1}	ΔF_g kJ/mol	σ_s mN/m
13.0	8.8	0.541	144.04	11.01	0.203	118.99	11.38
12.6	9.2	1.843	140.90	11.20	0.695	115.88	11.48
12.35	9.45	4.812	138.49	11.30	1.629	113.74	11.53
12.25	9.55	8.469	137.09	11.32	2.078	113.12	11.56

In Table 2 , the so derived values for J, ΔF_g, and σ_s for either volume or surface crystallization are given. As expected, ΔF_g is larger for the homogeneous case, whereas σ_s is similar in both cases. Both values are in good agreement with the literature value of σ_s = 11.8 mN/m given in refs 9 and 37. The lower ΔF_g in the surface case is compensated by the fact that fewer molecules can participate in forming this nucleus. Therefore, the freezing probability for both nucleation mechanisms is on the same order of magnitude, and heterogeneous nucleation at the surface layer cannot be excluded at this point.

3.3. Nucleation Mechanism. A more detailed inspection of these results allows us to distinguish if either homogeneous or heterogeneous nucleation is present. The best example is given in Figure 11 , which shows the ln(N_u/N_0) versus Vt plot for $C_{15}H_{32}$ at ΔT = 9.4 °C. This is the shortest alkane for which a surface layer has been observed. There is a strong deviation from the linear relationship according to eq 6. In a first approximation, the experimental graph may be described by two linear sections with different slopes. The first flat section represents a kind of induction time after which the nucleation process starts. That means that a preceding process in the supercooled liquid has to progress before a new, more probable nucleation mechanism may occur. It seems reasonable that the droplets injected at room temperature into the cold trap need some time to develop a solid, ordered surface layer. The freezing

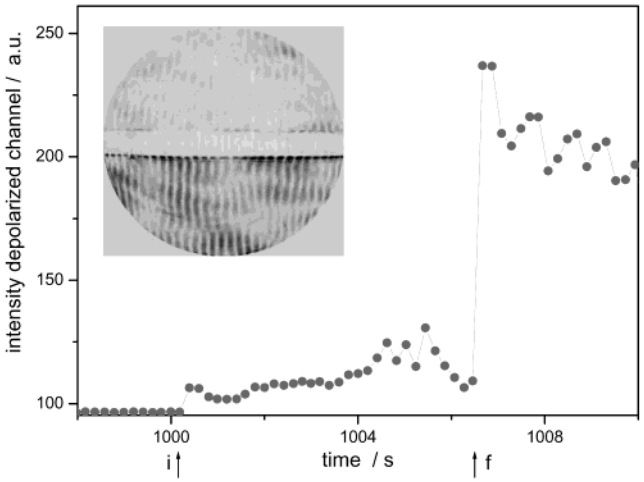

Figure 12. Increasing depolarization intensity with time for a $C_{15}H_{32}$ droplet before freezing. Inset: Typical scattering pattern during this induction time.

probability is obviously no longer constant but is a function of time. The experimental curve (Figure 11) can be fit by the solution of the differential equation

$$\frac{dN_u}{dt} = -(J_{hom}V_{hom} + J_{het}A_{het}(t)l_0)N_u \qquad (11)$$

The first term on the right side of this equation is related to nucleation in the bulk, and the second term describes nucleation at the surface layer. In this term, A_{het} is the area of the ordered surface layer. It grows between the times $t = 0$ and $t = t_0$, after which it reaches the limiting value A_{surf}. The law of growth can be expressed by

$$A_{het}(t) = A_{surf}\frac{t^n}{t_0} \qquad \text{for } t < t_0 \qquad (12)$$

A reasonable fit of the experimental curve is given by $2 \le n \le 3$. In Figure 11, the limiting cases of the fit curve are displayed. The case $n = 2$ means that the growth rate is proportional to the circumference of the surface layer (i.e., surface diffusion plays a dominant role), and $n = 3$ means that the growth rate is proportional to the area of the ordered layer (i.e., molecules from the bulk contribute to the growth). It is not possible to distinguish between these limiting cases. There are still other open questions in considering the formation of this surface phase. For the formation of this phase, a nucleation rate J_{surf}, which is not known, has to be postulated. The surface layer may be formed by several growing islands as a result of polynucleation. On the other side, sudden nucleation initiating the growth of a closed film cannot be excluded.

The presence of heterogeneous nucleation is supported by the observation of disturbances in the scattering pattern of the liquid droplet several seconds before the droplets freeze (Figure 12). The stripe pattern is superposed by intensity fluctuations, and the intensity of the depolarized, scattered light increases slightly with time. The stripes in the light-scattering pattern around the 90° scattering angle are predominantly produced by light traveling below the droplet surface. Since the penetration depth is only a few wavelengths of the scattered light, the observation of these disturbances point to a mostly liquid droplet with solid regions near the surface.

As shown in Figure 13, the observed induction times decrease with larger supercoolings with respect to the temperature T_l at which the surface layer is formed. The supercooling ΔT_l of

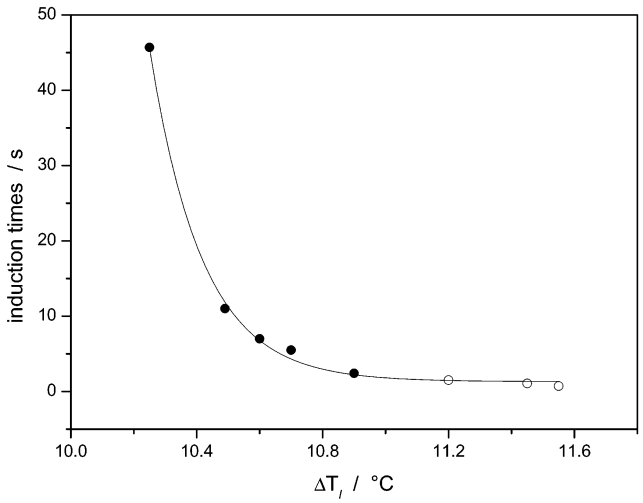

Figure 13. Temperature dependence of the induction times for $C_{15}H_{32}$ (●) and $C_{17}H_{36}$ (○). The supercooling temperature ΔT is given with respect to the temperature T_l at which the monolayer is formed.

TABLE 3: Nucleation Rates, ΔF_g, and σ_s of $C_{15}H_{32}$ Assuming Homogeneous and Heterogeneous Nucleation

		homogeneous			heterogeneous		
T_k °C	ΔT °C	J 10^5 cm^{-3} s^{-1}	ΔF_g kJ/mol	σ_s mN/m	J 10^{10} cm^{-3} s^{-1}	ΔF_g kJ/mol	σ_s mN/m
0.95	9.15	1.483	136.00	11.47	0.539	112.08	12.00
0.7	9.4	3.632	133.83	11.58	1.445	109.73	12.03
0.6	9.5	7.639	132.08	11.59	2.402	108.52	12.03
0.5	9.6	6.727	132.32	11.68	3.457	107.65	12.05
0.3	9.8	23.50	129.36	11.70	11.07	104.91	12.02

$C_{15}H_{32}$ ($T_l = 11.2$ °C) is smaller than the supercooling of $C_{17}H_{36}$ ($T_l = 23.8$ °C).[6] Therefore, the induction times for $C_{17}H_{36}$ are much shorter than those for $C_{15}H_{32}$.

Assuming heterogeneous nucleation at the surface layer, $J(\Delta T)$ for $C_{15}H_{32}$ was obtained by fitting a linear slope to the second part in the $\ln(N_u/N_0)$ versus Vt plots. The results are shown in Table 3. They are similar to the ones obtained for $C_{17}H_{36}$ at the same supercooling. $\Delta F_{act} = 16.0$ kJ/mol was estimated the same way as it was for $C_{17}H_{36}$. To evaluate σ_s, a value of $\Delta S = 0.506$ J/K cm^3 was interpolated from data for $C_{17}H_{36}$ and $C_{13}H_{28}$.[3] For σ_e, the value from $C_{17}H_{36}$ was taken. The so-derived values for σ_s are in good agreement with previous measurements.[9,37]

4. Conclusions

In this paper, we reported on freezing temperatures for supercooled *n*-alkane single droplets levitated in an electrodynamic trap. These droplets, which have an alkane/air interface, nucleate in the same temperature regions as smaller droplets in emulsions, where no solid monolayer at the interface is known to exist. We carried out a new experimental procedure to evaluate nucleation rates, and we could successfully apply it to $C_{15}H_{32}$ and $C_{17}H_{36}$ droplets. Similar values of J and σ_s for both chain lengths at the same supercoolings were obtained.

Experiments with levitated single droplets do not yield information only on supercooling temperatures and nucleation rates but also allow conclusions about the dynamic behavior of the nucleation process itself to be drawn. Large induction times observed for the $C_{15}H_{32}$ droplets indicate that the nucleation process takes place at the solid surface monolayer that has to be generated first. As pointed out, at the ordered solid surface layer, a kind of heterogeneous nucleation may take place. This

needs less activation energy for the formation of critical nuclei in comparison to that of homogeneous nucleation. Considering the freezing possibility of both processes, the lower activation energy of heterogeneous nucleation is compensated by a larger number of molecules participating in the homogeneous nucleation. Therefore, both mechanisms allow similar supercooling temperatures.

Acknowledgment. We thank E. Biller for technical support, H. Vortisch for the supply of computer software, and Dr. H. Riegler for helpful discussions regarding nucleation mechanisms. Financial support from the Deutsche Forschungsgemeinschaft (DFG) and the Fonds der Chemischen Industrie is gratefully acknowledged.

References and Notes

(1) Pruppacher, H. R.; Klett, J. D. *Microphysics of Clouds and Precipitation*, 2nd ed.; Kluwer Academic Publishers: Norwell, MA, 1997.

(2) Uhlmann D. R.; Kritchevsky, G.; Straff, R.; Scherer, G. *J. Chem. Phys.* **1975**, *62*, 4896.

(3) Oliver, M. J.; Calvert, P. D. *J. Cryst. Growth* **1975**, *30*, 343.

(4) Earnshaw, J. C.; Hughes, C. J. *Phys. Rev. A* **1992**, *46*, R4494.

(5) Wu, X. Z.; Sirota, E. B.; Sinha, S. K.; Ocko, B. M.; Deutsch, M. *Phys. Rev. Lett.* **1993**, *70*, 958.

(6) Wu, X. Z.; Ocko, B. M.; Sirota, E. B.; Sinha, S. K.; Deutsch, M.; Cao, B. H.; Kim, M. W. *Science (Washington, D.C.)* **1993**, *261*, 1018.

(7) Taggart, A. M.; Voogt, F.; Clydesdale, G.; Roberts, K. J. *Langmuir* **1996**, *12*, 5722.

(8) Sirota, E. B.; Herhold, A. B. *Science (Washington, D.C.)* **1999**, *283*, 529.

(9) Kraack, H.; Sirota, E. B.; Deutsch, M. *J. Chem. Phys.* **2000**, *112*, 6873.

(10) Kraack, H.; Deutsch, M.; Sirota, E. B. *Macromolecules* **2000**, *33*, 6174.

(11) Merkl, C.; Pfohl, T.; Riegler, H. *Phys. Rev. Lett.* **1997**, *79*, 4625.

(12) Ungar, G. *J. Phys. Chem.* **1983**, *87*, 689.

(13) Ewen, B.; Strobl, G. R.; Richter, D. *Faraday Discuss. Chem. Soc.* **1980**, *69*, 19.

(14) Snyder, R. G.; Macroncelli, M.; Qi, S. P.; Strauss, H. L. *Science (Washington, D.C.)* **1981**, *214*, 188.

(15) Doucet, J.; Denicolo, I.; Craievich, A. *J. Chem. Phys.* **1981**, *75*, 1523.

(16) Müller, A.; Lonsdale, K. *Acta Crystallogr.* **1948**, *1*, 129.

(17) Paul, W.; Steinwedel, H. *Z. Naturforsch.* **1953**, *8*, 448.

(18) Davis, E. J. *Aerosol Sci. Technol.* **1997**, *26*, 212.

(19) Kraemer, B.; Hübner, O.; Vortisch, H.; Leisner, T.; Schwell, M.; Ruehl, E.; Baumgärtel, H. *J. Chem. Phys.* **1999**, *111*, 6521.

(20) Stöckel, P.; Baumgärtel, H.; Vortisch, H.; Leisner, T. *J. Mol. Liq.* **2002**, *96-97*, 153−175.

(21) Baehr, H. O.; Stephan, K. *Wärme und Stoffübertragung*; Springer-Verlag: Berlin, 1994.

(22) Schwell, M.; Baumgärtel, H.; Weidinger, I.; Krämer, B.; Vortisch, H.; Leisner, T.; Rühl, E. *J. Phys. Chem. A* **2000**, *104*, 6726.

(23) Vortisch, H.; Krämer, B.; Weidinger, I.; Wöste, L.; Leisner, T.; Schwell, M.; Baumgärtel, H.; Rühl, E. *Phys. Chem. Chem. Phys.* **2000**, *2*, 1407.

(24) Aardahl, C. L.; Vehring, R.; Weber, R.; Schweiger, G.; Davis, E. J.; Wiedensohler, A. *J. Colloid Interface Sci.* **1997**, *192*, 228.

(25) Javaid, A.; Castle, G. S. P.; Inculet, I. I.; Shelstad, K. A.; Crum, G. W. *IEEE Trans. Ind. Appl.* **1980**, *IA-16*, 292.

(26) Hughes, J. F. *Electrostatic Particle Charging*; Wiley & Sons: New York, 1997.

(27) Sievert, U. Ph.D. Thesis, *Fachbereich Elektrotechnik*, Gerhard-Mercator-Universität-Gesamthochschule Duisburg, Duisburg, Germany, 1998.

(28) Mie, G. *Ann. Phys.* **1908**, *25*, 377.

(29) Bohren, C. F.; Huffmann, D. R. *Absorption and Scattering of Light by Small Particles*; Wiley-Interscience: New York, 1983.

(30) Kerker, M. *The Scattering of Light*; Academic Press: Oxford, U.K., 1969.

(31) Barber, P. W.; Chang, R. K. *Optical Effects Associated with Small Particles*; World Scientific: Singapore, 1988.

(32) Timmermas, J. *Physico-Chemical Constants of Pure Organic Compounds*; Elsevier Publishing Company: New York, 1950.

(33) Krämer, B.; Schwell, M.; Hübner, O.; Vortisch, H.; Leisner, T.; Rühl, E.; Baumgärtel, H.; Wöste, L. *Ber. Bunsen-Ges. Phys. Chem.* **1996**, *100*, 1911.

(34) Koop, Th.; Luo, B.; Biermann, U. M.; Crutzen, P. J.; Peter, Th. *J. Phys. Chem.* **1997**, *101*, 1117.

(35) Riegler, H. Private communication.

(36) Reid, R. C.; Prausnitz, J. M.; Poling, B. E. *The Properties of Gases and Liquids*, 4th ed; McGraw-Hill: Boston, MA, 1987.

(37) Wunderlich, B.; Arakawa, T. *J. Polym. Sci., Part A: Polym. Chem.* **1964**, *2*, 3697.

(38) To avoid confusion, this is a very high supercooling temperature compared to the average temperature given in Table 1. Almost all other droplets showed less supercooling.